Single-Mode Coherent Transmission over Universal Fiber for Data Center Interconnects

Fabio A. Barbosa[1*], **Mareli Rodigheri**[1,2], **Samuel Lennard**[1], **Ming-Jun Li**[3], **Filipe M. Ferreira**[1]
[1]*Optical Networks Group, Dept. Electronic & Electrical Eng., University College London (UCL), UK*
[2]*Faculty of Electrical and Computer Engineering, University of Campinas (UNICAMP), Brazil*
[3]*Science and Technology Division, Corning Incorporated, Corning, NY 14831*
**fabio.barbosa@ucl.ac.uk*

Abstract: We demonstrate DP-16-QAM up to 42 Gbaud over 50 km of universal fiber, meeting current DCI requirements while allowing SDM upgrades. Multipath interference is analyzed experimentally using mandrel wrapping and matched by split-step simulation. © 2024 The Authors

1. Introduction

The ever-increasing traffic demand in data centers calls for a scalable and cost-effective fiber cable infrastructure beyond the immediate increase in the number of optical fiber links, which may be too costly or of complex management [1]. Space-division multiplexing (SDM) is a potential candidate to support cost-efficient network capacity scaling that has recently been introduced in submarine cables using multi-core fibers (MCFs) [2-4]. Although for data centers, in which case inter-core crosstalk is not as severe, multimode fibers (MMFs) offer a different mix of advantages, such as direct connectivity to VCSELs or silicon photonic and InP photonic integrated circuits for high-degree integration and high-density interconnects, and there is no need to address the challenge of SDM amplification.

In this work, we explore a research fiber type that supports both multimode and single-mode transmission, the universal fiber [5, 6]. This is a MMF whose bandwidth is optimized for short wavelengths such as 850 nm. At the same time, the fundamental mode has a mode field diameter approximately matching that of a standard single-mode fiber (SMF) at 1310 and 1550 nm, which contributes to minimizing splicing losses or modal leakage to higher-order modes. By being compatible with both scenarios, the universal fiber type offers the prospect of taking full advantage of the cost and performance benefits of each fiber transmission type. In addition, the multimode nature of universal fiber could be attractive for SDM applications. This work investigates the transmission performance of the universal fiber when using (single mode) digital coherent transceivers, compare it to the transmission performance of SMFs, and quantify the residual penalty associated with multipath interference (MPI). MPI is analyzed experimentally using mandrel wrapping along the single span, to suppress the power leaked to higher-order modes, and through split-step numerical simulation using [7]. We aim to demonstrate that universal fiber can support data center interconnect (DCI) applications using single-mode transmission technology to meet current needs while providing a scalable path for future SDM upgrades. Furthermore, we explore the performance of conventional digital signal processing (DSP) techniques in the presence of MPI, including nonlinear compensation using digital backpropagation (DBP), and compare DSP equalizer taps requirements with those for conventional SMFs.

2. Experimental and experimental setup

The experimental setup used in this work is shown in Fig. 1. The signal of an external cavity laser (ECL) with 10 kHz linewidth was modulated using a dual-polarization (DP) IQ modulator, driven by 92 GS/s digital-to-analog converters (DACs). The drive signals consisted of 16-QAM signals, pulse-shaped using root raised cosine (RRC) filters with 0.1 roll-off, at symbol rates of 21 and 42 Gbaud. To perform channel estimation, 2 consecutive constant amplitude zero autocorrelation (CAZAC) training sequences (TS) with length of 4096 symbols preceded the payload. Shorter TSs could have been chosen with no considerable performance loss (see Fig. 5), but the length of the TS employed here enables to capture and investigate more broadly channel impulse response artifacts. For carrier phase recovery (CPR) purposes, QPSK pilot symbols were added at a rate of P = 1/32. Digital pre-emphasis was applied to the signal to compensate for the frequency response of the transmitter components [8]. An Erbium-doped fiber amplifier (EDFA)

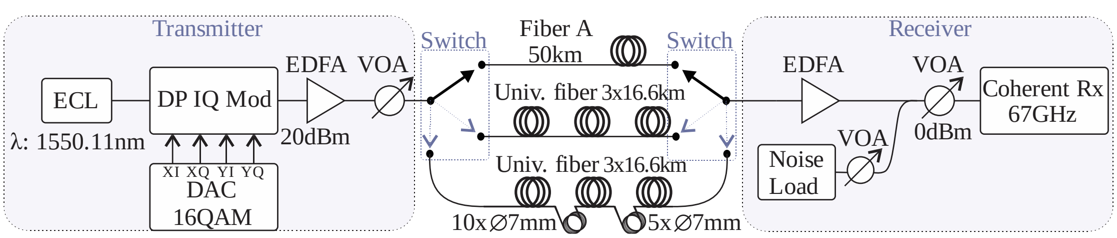

Fig. 1. Schematic diagram of the optical transmission system.

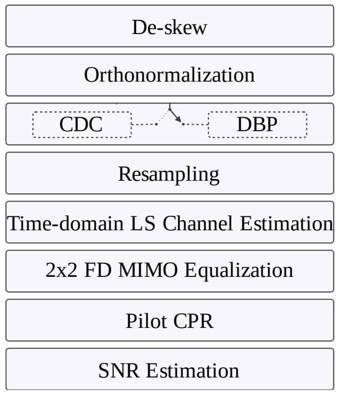

Fig. 2 Chain of DSP stages used to process the experimentally collected traces.

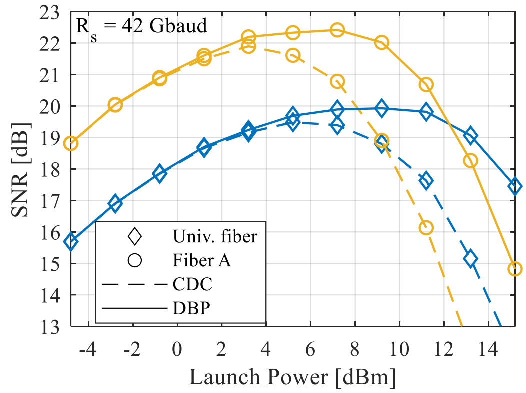

Fig. 3 SNR as a function of launch power for experimental transmission of DP-16QAM at 42 Gbaud over 50 km of univ. fiber and Fiber A, including results with and without DBP.

followed by a variable optical attenuator (VOA) was used to control the signal launch power, and a single fiber span of approximately 50 km was tested. The fibers used are specified later in this section. A second EDFA was used to compensate for link losses as well as to set a constant power level of 0 dBm, in combination with a VOA, to the coherent receiver. EDFAs in this experiment have a noise figure of ~5.5 dB. Additionally, an amplified spontaneous emission loading stage was used to increase the noise floor and set the link optical signal-to-noise ratio (OSNR).

A DP coherent receiver with 67-GHz electrical bandwidth balanced photodetectors was employed. Homodyne detection was considered using the same 10-kHz-linewidth ECL as transmitter and local oscillator (LO) laser. The received signals were then digitized with a real-time digital sampling oscilloscope of 110 GHz electrical analog bandwidth at 256 Gsamples/s and processed off-line. The off-line digital signal processing (DSP) chain is illustrated in Fig. 2. It includes de-skew, orthonormalization, chromatic dispersion compensation (CDC), resampling to 2 samples/symbol, channel estimation, MIMO equalization, and pilot CPR. In this work, the 2×2-MIMO channel is estimated using a time-domain least-square (LS) approach [9]. Importantly, the estimated channel impulse response (CIR) is truncated to L taps, a parameter varied to investigate equalization requirements for the different fiber types (see Fig. 5). Then, after zero-padding, the L-tap (truncated) estimate CIRs are converted to frequency domain (FD) and used for zero-forcing (ZF) equalization. The overlap-save method is used with 4096-point FFTs and overlap of 128 samples. The received traces were also processed using (single mode) DBP to gain insight on whether MPI would have an impact on DBP. In this scenario, the CDC stage was replaced by the DBP implemented using the split-step Fourier method (SSFM) (see Fig. 2). The effective signal-to-noise ratio (SNR) of received constellations was used as performance metric in this work, namely: $E[|X|^2]/E[|X-Y|^2]$, where X and Y are the transmitted and received symbols after DSP is applied, respectively.

Here, two different fibers are considered, namely a 50 km research universal fiber with ~30 µm core diameter [6], consisting of 3 directly spliced spools of ~16.6 km and a 50 km regular effective area (82 µm^2) single-mode fiber with ultra-low loss (Fiber A). Note that the Fiber A was chosen to reflect the state-of-the-art, single-mode fibers available today. It was used in this experiment for system performance comparison only as it has lower attenuation. For the universal fiber, standard SMF pigtails of ~1-m were used. Investigations with the universal fiber also included the use of mandrel wrapping (MW), which consisted of wrapping the fiber 10 times around a 7-mm mandrel at length 16.6 km and 5 times at length 33.3 km (see Fig. 1). This scenario is indicated by univ. fiber + MW. The noise loading was set once to obtain a OSNR of 29 dB/0.1nm for Fiber A and left unchanged for all other experiment scenarios.

3. Results and Discussions

The received SNR as a function of launch power for the universal fiber and Fiber A is shown in Fig. 3, for a symbol rate of 42 Gbaud, without and with DBP. A fixed number of L=31 taps was used for the estimated CIR with both fibers. The SNR at optimum launch power is 2.4 dB smaller for the universal fiber – this SNR difference is due to MPI and will be further explored later on here. Also, the SNR curve for the universal fiber is shifted towards higher launch power given its higher attenuation. Furthermore, Fig. 3 shows that DBP provides a similar gain of ~0.5 dB for both fiber scenarios. Here, the DBP parameters were optimized for each fiber, excluding the number of fiber steps which was fixed in 10 steps. Note that DBP gains are limited due to the single span scenario and by the transceiver noise at optimum launch power [10].

Fig. 4 shows the received SNR as a function of launch power for a second set of results with the universal fiber, including mandrel wrapping (see Fig. 1). It can be observed that the SNR performance remains similar in the linear and nonlinear regimes, while the performance at optimum launch power improves by 1.4 dB with the mandrel

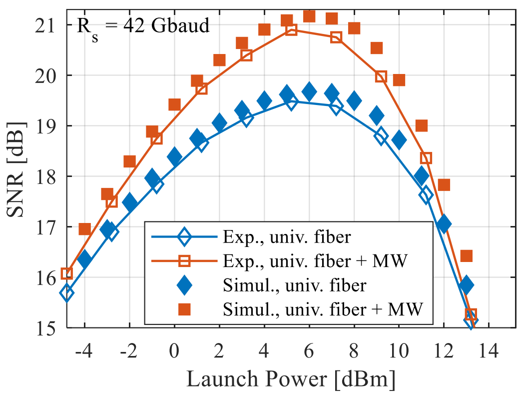

Fig. 4 SNR vs launch power for DP-16QAM at 42 Gbaud over 50-km univ. fiber, with and without mandrel wrapping. Experimental (lines with markers) and simulation (only markers) results included.

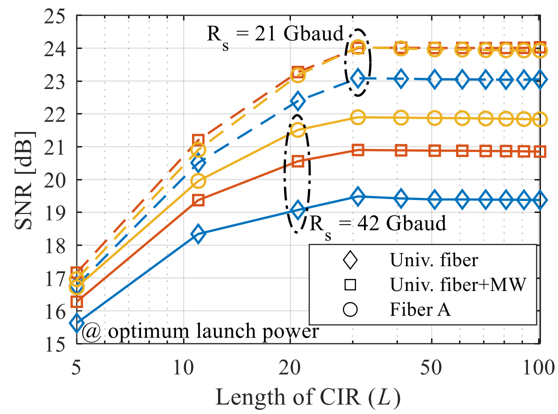

Fig. 5. SNR vs length of (estimated) CIR (L) used for equalization of experimental transmission of DP-16-QAM, at 21 and 42 Gbaud, over 50 km of univ. fiber, univ. fiber+MW or Fiber A, at optimum launch power (without DBP).

wrapping. This performance differential is the result of MPI – this is, leakage of optical power from the fundamental mode into higher-order modes that then couples back to the fundamental mode. The results show that tight fiber wrapping, 10 turns of 7 mm diameter at 16.6 km and 5 turns of 7 mm diameter at 33.3 km, reduces the MPI induced penalty by introducing significant bending loss to the higher order modes while having minimal impact on the fundamental mode which is strongly guided and whose mode field distribution is well confined to the fiber core. Following the approach in [11], we estimated the macro-bending loss (MBL) for the 2nd mode group to be 0.05 dB per turn and for the 3rd mode group to be 3.3 dB per turn. Also shown in Fig. 4 are results of transmission simulations assuming a fiber with characteristics similar to those of the universal fiber and using the model in [7]. By adjusting the crosstalk (XT) level in dB/km, the simulations results were matched to the universal fiber experimental results. The best fit was obtained with a XT of -34 dB/km. For the case with mandrel wrapping, in simulation, the optical signals in the 2nd and 3rd mode groups were attenuated by 0.05 dB/turn and 3.3dB/turn, respectively, at 16.6 km and 33.3 km – higher-order mode groups were fully stripped. A good agreement can be observed between the experimental and simulation results. We noted that the MPI between the fundamental mode and 2nd mode group is dominant and not fully removed by mandrel wrapping for a MBL of 0.05 dB/turn.

The SNR results as a function of the CIR length L used for equalization are shown in Fig. 5, at optimum launch power (without DBP) for the rates of 21 and 42 Gbaud. In all cases L = 31 taps is optimal. At 21 Gbaud, the SNR performance of Fiber A and univ. fiber are similar when using MW – in this case, MW improves SNR by 1 dB at optimal L (31 taps). Finally, note that the larger the symbol rate, the larger the MPI penalty is, 1 dB and 2.4dB at 21 Gbaud and 42 Gbaud, respectively. This can be explained by the combined effect of MPI and modal dispersion.

4. Conclusions

We demonstrated that DP-16-QAM transmission up to 42 Gbaud over 50-km universal fiber can be achieved with a small SNR penalty (1-2 dB) to standard SMFs. This confirms that universal fiber can support DCI applications using single-mode transmission to meet current needs, while providing a scalable path for future SDM upgrades.

This work was supported in part by the UKRI Future Leaders Fellowship under Grant MR/T041218/1, the Strategic Equipment under Grant EP/V007734/1, and São Paulo Research Foundation under grant 2023/03732-4. For the underlying data, see: doi.org/10.5522/04/24428188.

5. References

[1] C. Xie and B. Zhang, "Scaling Optical Interconnects for Hyperscale Data Center Networks," *Proc. IEEE*, vol. 110, no. 11, p. 1699-1713, 2022.
[2] W. Klaus, *et al.*, "The Role of Parallelism in the Evolution of Optical Fiber Communication Systems," *IEEE*, vol. 110, no. 11, pp. 1619-1654, 2022.
[3] J. D. Downie, *et al.*, "Modeling the Techno-Economics of Multicore Optical Fibers in Subsea Transmission Systems," *J. Light. Technol.*, vol. 40, no. 6, pp. 1569-1578, 2022.
[4] B. Quigley and M. Cantono. "Boosting Subsea Cables with Multi-Core Fiber Technology." https://cloud.google.coms (accessed 15th Oct., 2023).
[5] X. Chen, *et al.*, "Design of universal fiber with demonstration of full system reaches over 100G SR4, 40G sWDM, and 100G CWDM4 transceivers," *Optics Express*, vol. 24, no. 16, pp. 18492-18500, 2016.
[6] X. Chen, *et al.*, "Universal Fiber for Short-Distance Optical Communications," *J. Light. Technol.*, vol. 37, no. 2, pp. 389-395, 2019.
[7] F. Ferreira, *et al.*, "Semi-Analytical Modelling of Linear Mode Coupling in Few-Mode Fibers," *J. Light. Technol.*, vol.35, no.18, pp. 4011-4022, 2017.
[8] B. Geiger, *et al.*, "On the Performance Limits of High-Speed Transmission Using a Single Wideband Coherent Receiver," *J. Light. Technol.*, vol. 41, no. 12, pp. 3816-3824, 2023.
[9] M. Kuschnerov, *et al.*, "Data-Aided Versus Blind Single-Carrier Coherent Receivers," *IEEE Photonics Journal*, vol. 2, no. 3, pp. 387-403, 2010.
[10] L. Galdino, *et al.*, "On the limits of digital back-propagation in the presence of transceiver noise," *Opt. Express*, vol. 25, no. 4, pp. 4564-4578, 2017.
[11] K. S. Kaufman, *et al.*, "Curvature loss in multimode optical fibers," *J. Opt. Soc. Am.*, vol. 71, no. 12, pp. 1513-1518, 1981.